Spectroscopic study of laser-induced tunneling ionization of nitrogen molecules

Peng Wang,[1] Shaohua Xu,[1] Donghai Li,[1] Hong Yang,[1] Hongbing Jiang,[1] Qihuang Gong,[1,2] and Chengyin Wu[1,2,*]
[1]*Department of Physics, State Key Laboratory for Mesoscopic Physics, Peking University, Beijing 100871, China*
[2]*Collaborative Innovation Center of Quantum Matter, Beijing, China*
(Received 1 July 2014; published 10 September 2014)

Tunneling ionization is one of the fundamental processes for molecules in intense laser fields. Depending on the ionizing molecular orbitals, molecular ions are in ground or excited electronic states. Here, we report an experimental study of tunneling ionization of nitrogen molecules using spectroscopic methods. The molecular ions in the excited electronic state were detected through the fluorescence spectra. The molecular ions in the ground electronic state were detected through the laser-induced-fluorescence (LIF) spectra. The gas-pressure dependences of fluorescence and LIF intensities demonstrated the collision-induced population redistribution in these electronic states.

DOI: 10.1103/PhysRevA.90.033407 PACS number(s): 33.80.Rv, 42.50.Hz, 33.20.Xx

I. INTRODUCTION

The laser-molecule interaction is very complicated in intense laser fields [1]. There are many reaction channels for molecules irradiated by intense laser pulses. Among them tunneling ionization is the fundamental process in which a correlated electron and a parent ion are generated. Driven by the oscillating laser field, the electron might recollide with the parent ion and trigger other strong-field phenomena [2], such as above-threshold ionization [3], high-order harmonic generation [4], nonsequential double ionization [5], laser-induced electron diffraction [6], as well as excitation and dissociation of molecular ions [7,8]. Various experimental techniques have been developed to explore these dynamic processes. Cold target recoil ion momentum spectroscopy (COLTRIMS) has the capability of high momentum resolution, full solid angle collection, and coincidence measurement [9]. It can measure the yields and momentum vectors of ions and electrons produced in the tunneling ionization and has become a powerful tool to study tunneling ionization of molecules in intense laser fields. But this technique is not sensitive to the internal quantum state of molecular ions, such as electronic states. Considering the ionization rate decays exponentially on the electron binding energy, it is always assumed that the electron in the highest occupied molecular orbital (HOMO) is first removed by the laser electric field and the molecular ion is therefore in the ground electronic state. However, recent experimental observations demonstrated that multiple orbitals involved in the process of tunneling ionization and molecular ions are in various electronic states [10,11].

As the major components of air, the interaction between pure nitrogen molecules and intense laser fields has been extensively studied both experimentally and theoretically [12–26]. According to the molecular Ammosov-Delone-Krainov (MO-ADK) model [27], the ionization rate is determined not only by the electron binding energy, but also by the symmetry of the ionizing molecular orbital. For neutral nitrogen molecules, the electronic configuration is $KK(\sigma_g 2s)^2(\sigma_u 2s)^2(\pi_u 2p)^4(\sigma_g 2p)^2$. The binding energies are 15.58, 17.07, and 18.75 eV for HOMO (σ_g), HOMO-1(π_u), and HOMO-2 (σ_u), respectively. Because of the small energy differences and different symmetries, multiple orbitals are simultaneously involved in the process of tunneling ionization, and molecular ions are in various electronic states. Based on the molecular orbital theory, removal of one electron from HOMO, HOMO-1, and HOMO-2 of N_2 leaves N_2^+ in the electronic states of $X\ ^2\Sigma_g^+$, $A\ ^2\Pi_u$, and $B\ ^2\Sigma_u^+$, respectively. Pavičić *et al.* aligned some linear molecules and then measured the ion yield as a function of alignment angle. The angle-dependent ionization probabilities were therefore obtained for nitrogen, oxygen, and carbon dioxide molecules in an intense laser field [21]. However these measurements were taken in the apparatus of COLTRIMS, which cannot judge the internal quantum state of ions. Considering the ionization rate decays exponentially in the electron binding energy, Pavičić *et al.* assumed that the HOMO electron is first removed by the laser electric field and the molecular ion is in the ground electronic state. Thus they concluded that the observed molecular ions result from the tunneling ionization of the HOMO electron and the measured angle-dependent ionization probability reflects the symmetry of the HOMO. But a closer inspection of the angle-dependent ionization probability reveals some discrepancies between the experimental measurements and the MO-ADK predictions. The disagreement was improved when multiple orbital contributions were included [25]. Soon, the alignment-dependent structure observed in the high-order harmonic spectra provided direct experimental evidence that nitrogen molecules can be ionized through tunneling from HOMO and HOMO-1 simultaneously [28,29]. Unfortunately, sophisticated theories are required to interpret high-order harmonic spectra, especially to disentangle the orbital contributions. The fluorescent spectroscopy can determine the electronic state through observing the fluorescence emission when the molecular ion is in the excited electronic state. The observation of $N_2^+(B\ ^2\Sigma_u^+ \rightarrow X\ ^2\Sigma_g^+)$ demonstrated the generation of N_2^+ in the excited electronic state of $B\ ^2\Sigma_u^+$ and indicated that HOMO-2 is involved in the tunneling ionization process [30]. However, a population inversion was recently demonstrated between $N_2^+(B\ ^2\Sigma_u^+)$ and $N_2^+(X\ ^2\Sigma_g^+)$ by observing the lasinglike emission between these two electronic states of N_2^+ [31–37]. Because such cavityless laser sources

*cywu@pku.edu.cn

have the great potential for remote sensing applications, the realization of the N_2^+ laser has been extensively studied. The coherent narrow-bandwidth lasing emission around 391 nm in the forward direction was realized first in the presence of a seed pulse [31–35]. Very soon, such forward lasing emission was realized by a single 800-nm femtosecond laser pulse [36,37]. However, the lasing lines shifted from 391 to 428 nm as the gas pressure increased [37]. These two lasing lines correspond to the transitions of $N_2^+(B\ ^2\Sigma_u^+, v' = 0 \rightarrow X\ ^2\Sigma_g^+, v'' = 0)$ and $N_2^+(B\ ^2\Sigma_u^+, v' = 0 \rightarrow X\ ^2\Sigma_g^+, v'' = 1)$, respectively. The authors attributed the observed lasing lines around 391 and 428 nm to a self-seeding effect. Even though there is no doubt for the population inversion between $N_2^+(B\ ^2\Sigma_u^+)$ and $N_2^+(X\ ^2\Sigma_g^+)$, the mechanism responsible for the population inversion is still in debate.

In this article, we experimentally studied the tunneling ionization of nitrogen molecules irradiated by intense femtosecond laser fields. The electronic states of N_2^+ were identified using spectroscopic methods. The populations of $N_2^+(B\ ^2\Sigma_u^+)$ and $N_2^+(X\ ^2\Sigma_g^+)$ were explored by measuring the fluorescence spectra and the LIF spectra, respectively. The ratio of the LIF intensity to the fluorescence intensity was obtained as a function of gas pressure. The results demonstrated the collision-induced population redistribution should be taken into account when exploring the population inversion between $N_2^+(B\ ^2\Sigma_u^+)$ and $N_2^+(X\ ^2\Sigma_g^+)$ observed in the interaction of nitrogen molecules and intense laser fields.

II. EXPERIMENTAL SETUP

The experimental setup of fluorescence spectroscopy has been described in our previous paper [38]. Here, we modified the fluorescence spectroscopy and added the function of LIF measurement. A femtosecond laser amplifier (TSA-10, Spectra-Physics, USA) and a nanosecond tunable laser (NT342B-SH/SFG-10, Lithuania) were used in the current experiments. The femtosecond laser delivers laser pulses with a central wavelength of 800 nm and a pulse duration of 110 fs at a repetition rate of 10 Hz. The nanosecond laser has a broad wavelength tunable range between 225 and 2600 nm. The typical pulse duration is 3–5 ns. The linewidth is narrower than 8 cm^{-1} in the range of 225–410 nm and 5 cm^{-1} in the range of 410–2600 nm. The femtosecond laser pulses were focused into the chamber filled with pure nitrogen molecules by using a convex lens ($f = 200$ mm). The gaseous nitrogen molecules were introduced into the chamber via a pulsed valve (Park, Inc., USA) with a 0.2-mm orifice. The vacuum chamber was pumped by a magnetically levitated molecular turbopump backed by a dry scroll pump. The base pressure can reach 3×10^{-7} mbar. It should be mentioned that the supersonic molecular beam was applied only in the measurement with the gas pressure lower than 1.0×10^{-4} mbar. When the gas pressure was beyond this range, the vacuum chamber was utilized as a static gas cell. The peak intensity of the laser pulse was estimated by measuring pulse energy, pulse duration, and focusing size. Tunneling ionization is the fundamental process for nitrogen molecules irradiated by intense femtosecond laser fields. The N_2^+ ions in the excited electronic state were detected by measuring the fluorescence emission from the excited electronic state to the ground electronic state. The N_2^+ ions in the ground electronic state were detected by measuring the LIF emission in which a nanosecond laser was applied to populate the molecular ion from the ground electronic state to the excited electronic state, and then the fluorescence emission from the excited electronic state to the ground electronic state was scanned. In the LIF experiment, the femtosecond laser and the nanosecond laser were set to counterpropagate. The delay time between the two lasers was controlled by a delay generator (Stanford Research, DG535). A combination of one spherical mirror and one convex lens was applied to improve the fluorescence collection efficiency. Then the fluorescence light was focused into a monochromator followed by a photomultiplier tube (PMT). The output analog signals of the PMT were sent to a 2-GHz dual-channel data-acquisition card (CS22G8, GAGE, USA) and were recorded by a computer for storage and analysis.

III. RESULTS AND DISCUSSION

Figure 1 shows the fluorescence spectra of pure nitrogen molecules irradiated by intense laser pulses at three different gas pressures (a) 1.4×10^{-5} mbar, (b) 2.5×10^{-1} mbar, and (c) 1.0×10^3 mbar. The laser had a pulse duration of 110 fs, a central wavelength of 800 nm, and an intensity of a few 10^{15} W/cm^2. The spectra were recorded over the wavelength range of 320–440 nm and were not

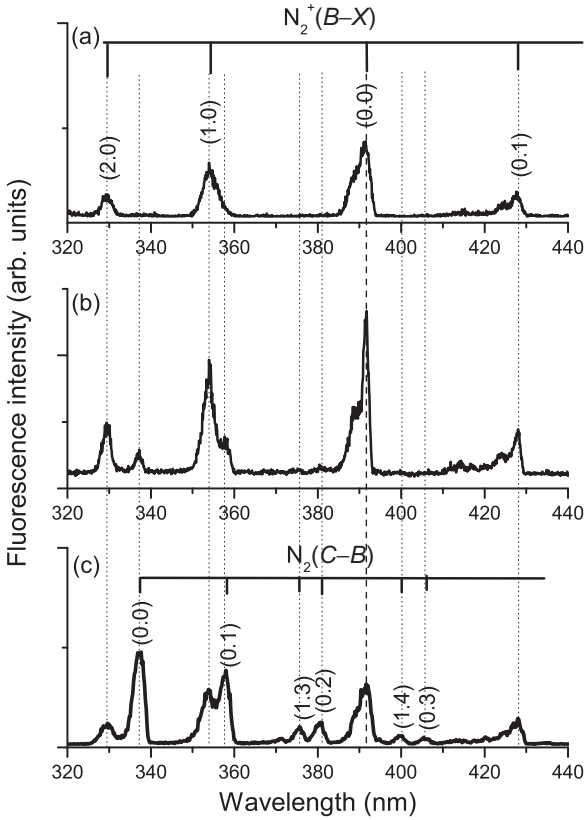

FIG. 1. Fluorescence spectra of pure nitrogen molecules irradiated by intense laser pulses at three different gas pressures (a) 1.4×10^{-5} mbar, (b) 2.5×10^{-1} mbar, and (c) 1.0×10^3 mbar. The laser has a pulse duration of 110 fs, a central wavelength of 800 nm, and an intensity of a few 10^{15} W/cm^2.

calibrated by the wavelength response of the fluorescence detection system. When the gas pressure is 1.0×10^3 mbar, the spectra can be assigned to $N_2(C\ ^3\Pi_u \rightarrow B\ ^3\Pi_g)$ and $N_2^+(B\ ^2\Sigma_u^+ \rightarrow X\ ^2\Sigma_g^+)$, which are consistent with a previous paper [39]. The emission of $N_2(C\ ^3\Pi_u \rightarrow B\ ^3\Pi_g)$ gradually became weak with decreasing the gas pressure. When the gas pressure was 1.4×10^{-5} mbar, the emission of $N_2(C\ ^3\Pi_u \rightarrow B\ ^3\Pi_g)$ completely disappeared, and only the emission of $N_2^+(B\ ^2\Sigma_u^+ \rightarrow X\ ^2\Sigma_g^+)$ was observed. The numbers in the parentheses (v',v'') denoted the vibrational levels of the upper and the lower electronic states. The (0,0) bands locate at 337.0 and 391.1 nm for $N_2(C\ ^3\Pi_u \rightarrow B\ ^3\Pi_g)$ and $N_2^+(B\ ^2\Sigma_u^+ \rightarrow X\ ^2\Sigma_g^+)$, respectively.

There are many reaction channels when pure nitrogen molecules are subject to intense femtosecond laser fields, among which tunneling ionization is the initial process. The formed N_2^+ ions are in various electronic states because of the involvement of multiple orbitals. The excited electronic states can be identified through fluorescence spectra, and the ground electronic state can be identified through LIF spectra. In the case of LIF spectra, a tunable nanosecond laser populated N_2^+ from the ground electronic state $X\ ^2\Sigma_g^+$ to the excited electronic state $B\ ^2\Sigma_u^+$, and then the fluorescence emission of $N_2^+(B\ ^2\Sigma_u^+ \rightarrow X\ ^2\Sigma_g^+)$ was scanned. In order to separate the fluorescence and the LIF, the nanosecond laser lagged behind the femtosecond laser 200 ns. Figure 2 shows the fluorescence spectra of $N_2^+(B\ ^2\Sigma_u^+)$ and the LIF spectra of $N_2^+(X\ ^2\Sigma_g^+)$ in which N_2^+ were generated through ionization of pure nitrogen molecules by 110-fs 800-nm laser pulses at an intensity of a few 10^{15} W/cm^2. The fluorescence spectra shown in Fig. 2(a) can be assigned to $N_2^+(B\ ^2\Sigma_u^+, v' = 0-2 \rightarrow X\ ^2\Sigma_g^+, v'' = 0-2)$. Figures 2(b) and 2(c) show the LIF spectra of $N_2^+(X\ ^2\Sigma_g^+, v'' = 0)$. In Fig. 2(b), the nanosecond laser was set at 391.5 nm to populate N_2^+ from $X\ ^2\Sigma_g^+(v'' = 0)$ to $B\ ^2\Sigma_u^+(v' = 0)$, and the fluorescence of $N_2^+(B\ ^2\Sigma_u^+, v' = 0 \rightarrow X\ ^2\Sigma_g^+, v'' = 1,2)$ was observed. In Fig. 2(c), the nanosecond laser was set at 358.2 nm to populate N_2^+ from $X\ ^2\Sigma_g^+(v'' = 0)$ to $B\ ^2\Sigma_u^+(v' = 1)$, and the fluorescence of $N_2^+(B\ ^2\Sigma_u^+, v' = 1 \rightarrow X\ ^2\Sigma_g^+, v'' = 1,2)$ was observed. The LIF spectra further confirmed the assignment of the fluorescence spectra shown in Fig. 2(a).

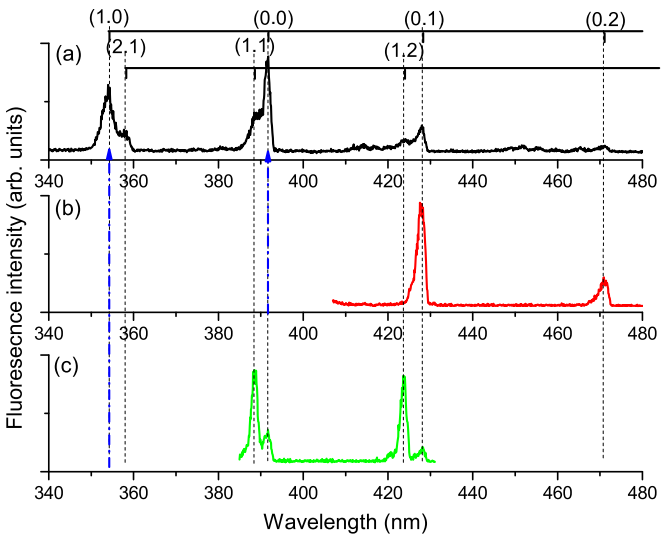

FIG. 2. (Color online) (a) Fluoresce spectra and (b) and (c) LIF spectra of pure nitrogen molecules irradiated by 110-fs 800-nm laser pulses at an intensity of a few 10^{15} W/cm^2. The wavelength of the nanosecond laser was set at (b) 391.5 nm and (c) 358.2 nm and was represented by the blue dashed-dotted lines (see text).

The LIF intensity is proportional to the vibrational population of $N_2^+(X\ ^2\Sigma_g^+, v'')$, the Franck-Condon factor of excitation transition and fluorescence emission, as well as the fluorescence detecting efficiency. In the following, we give an example to show how to determine the relative vibrational population of $N_2^+(X\ ^2\Sigma_g^+, v'')$ based on the LIF measurement. When exploring the population of $N_2^+(X\ ^2\Sigma_g^+, v'' = 0)$, we set the nanosecond laser at 391.5 nm to populate N_2^+ from $X\ ^2\Sigma_g^+(v'' = 0)$ to $B\ ^2\Sigma_u^+(v' = 0)$ and the LIF wavelength at 427.8 nm to collect the fluorescence emission of $N_2^+(B\ ^2\Sigma_u^+, v' = 0 \rightarrow X\ ^2\Sigma_g^+, v'' = 1)$. When exploring the population of $N_2^+(X\ ^2\Sigma_g^+, v'' = 1)$, the nanosecond laser was set at 388.5 nm to populate N_2^+ from $X\ ^2\Sigma_g^+(v'' = 1)$ to $B\ ^2\Sigma_u^+(v' = 1)$, and the LIF wavelength was set at 423.9 nm to collect the fluorescence emission of $N_2^+(B\ ^2\Sigma_u^+, v' = 1 \rightarrow X\ ^2\Sigma_g^+, v'' = 2)$. By comparing the LIF intensities, the ratio of the population at $v'' = 0$ to that at $v'' = 1$ was determined to be 3.6 after the corrections of Franck-Condon factors. Here we neglected the difference of the pumping efficiency caused by the energy fluctuation of the nanosecond laser at 391.5 and 388.5 nm as well as the difference in fluorescence detection efficiency at 427.8 and 423.9 nm. It should be mentioned that the measurement was taken at the gas pressure of 1.0 mbar. At this gas pressure, collision-induced population redistribution cannot be neglected. Thus the ratio of 3.6 cannot represent the initial population ratio of $N_2^+(X\ ^2\Sigma_g^+, v'' = 0)$ to $N_2^+(X\ ^2\Sigma_g^+, v'' = 1)$.

To study the impact of collision on the population redistribution quantitatively, we measured the pressure-dependent fluorescence decay curves, which were characterized by fluorescence lifetimes at different gas pressures. The fluorescence collecting at 427.8 nm represented the emission of $N_2^+(B\ ^2\Sigma_u^+, v' = 0 \rightarrow X\ ^2\Sigma_g^+, v'' = 1)$ and was generated through ionization of pure nitrogen molecules by an intense femtosecond laser field. The results were displayed in Fig. 3, and the fluorescence lifetimes were obtained through fitting the experimental data with an exponential decay function and were represented by the black solid lines. It can be seen that the fluorescence lifetime became shortened with increasing the gas pressure. The pressure-dependent fluorescence lifetime can be explained by the collision-induced depopulation of the excited electronic state. It is known that the fluorescence lifetime refers to the average time the molecule stays in its excited state before emitting a photon. Various radiative and nonradiative processes can depopulate the excited state. The fluorescence lifetime τ, the radiative lifetime $\tau_{\rm rad}$, and the nonradiative lifetime $\tau_{\rm nrad}$ have the relationship $\frac{1}{\tau} = \frac{1}{\tau_{\rm rad}} + \frac{1}{\tau_{\rm nrad}}$. The radiative lifetime $\tau_{\rm rad}$ of $N_2^+(B\ ^2\Sigma_u^+ \rightarrow X\ ^2\Sigma_g^+)$ is around 60 ns [30]. The nonradiative lifetime $\tau_{\rm nrad}$ is mainly determined by the collision time between molecules. The mean

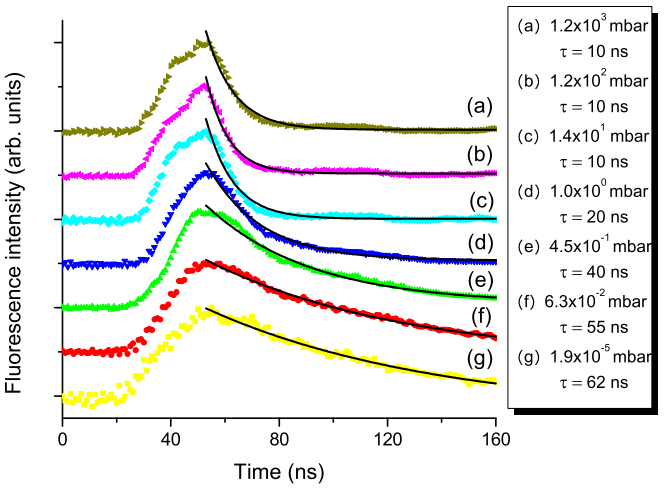

FIG. 3. (Color online) Fluorescence lifetimes of $N_2^+(B\ ^2\Sigma_u^+, v' = 0 \rightarrow X\ ^2\Sigma_g^+, v'' = 1)$ at different gas pressures. The fluorescence lifetimes were obtained through fitting the experimental data with an exponential decay function, which are represented by the black solid lines.

collision time for nitrogen molecules can be described by $t = \lambda/v \propto 1/P$, where λ and v are the mean path and the average speed of nitrogen molecules at room temperature and P is the gas pressure. It is obvious that the mean collision time is inversely proportional to the gas pressure. When the gas pressure is 1.0 mbar, the mean collision time is 160 ns. In comparison with the radiative lifetime, the collision-induced nonradiative processes cannot be neglected for depopulating the excited state at gas pressures higher than 10^{-2} mbar. According to the measurement, the fluorescence lifetime was 62 ns when the gas pressure was 1.9×0^{-5} mbar. The value was very close to the radiative lifetime of $N_2^+(B\ ^2\Sigma_u^+ \rightarrow X\ ^2\Sigma_g^+)$. The closeness of the fluorescence lifetime and the radiative lifetime indicated that the collision-induced nonradiative process can be neglected and the fluorescence lifetime was mainly determined by the radiative lifetime. This observation agrees with the expectation of a long mean collision time at low gas pressures. When the gas pressures were between 10^{-2} and 10^1 mbar, the fluorescence lifetime was very sensitive to the gas pressure. It decreased from about 55 to 10 ns when the gas pressures increased from 6.3×10^{-2} to 1.4×10^1 mbar. The observation can be explained by the fact that the mean collision time is comparable to the radiative lifetime when the gas pressure is in the above-mentioned range. Thus the fluorescence lifetime has a sensitive dependence on the gas pressure. When the gas pressure was higher than 1.4×10^1 mbar, the mean collision time was shorter than 10 ns. Thus the nonradiative lifetime caused by the collision was much shorter than the radiative lifetime. Therefore, the fluorescence lifetime was determined by the mean collision time. However, the time resolution of our fluorescence measurement system was 10 ns. The fluorescence lifetime approached the time resolution when the gas pressure was higher than 1.4×10^1 mbar, which was consistent with our measurements again.

Tunneling ionization is the initial process for N_2 in intense femtosecond laser fields. The involvement of multiple orbitals in the process of tunneling ionization generates N_2^+ in various electronic states. Removal of one electron from HOMO, HOMO-1, and HOMO-2 of N_2 leaves N_2^+ in the electronic states of $X\ ^2\Sigma_g^+, A\ ^2\Pi_u$, and $B\ ^2\Sigma_u^+$, respectively. When the N_2^+ ion is in the excited electronic state, the fluorescent spectroscopy can determine the electronic state through observing the fluorescence emission. The present observation of $N_2^+(B\ ^2\Sigma_u^+ \rightarrow X\ ^2\Sigma_g^+)$ demonstrated the generation of N_2^+ in the excited electronic state of $B\ ^2\Sigma_u^+$ and indicated that HOMO-2 is involved in the tunneling ionization process. The absence of $N_2^+(A\ ^2\Pi_u \rightarrow X\ ^2\Sigma_g^+)$ emission was due to the fact that this emission locates at the infrared regime [40] and is beyond the spectral response of our fluorescence detection system. The LIF spectra confirmed the generation of $N_2^+(X\ ^2\Sigma_g^+)$. Therefore, the combination of fluorescence spectra and LIF spectra can determine the electronic state, whether the molecular ion is in the excited electronic state or in the ground electronic state. As a result, the tunneling ionization contributions can be disentangled for different molecular orbitals. Because the fluorescence and the LIF intensities, respectively, were proportional to the population of $N_2^+(B\ ^2\Sigma_u^+)$ and $N_2^+(X\ ^2\Sigma_g^+)$, it is expected that the ratio of the fluorescence to the LIF is determined only by the laser parameters if the initial populations of $N_2^+(B\ ^2\Sigma_u^+)$ and $N_2^+(X\ ^2\Sigma_g^+)$ are not affected by the collision. However, we observed that the ratio strongly depended on gas pressures. Figure 4 shows the fluorescence and the LIF intensities at various gas pressures. The intensities have been normalized with the fluorescence intensity. In the measurement, the nanosecond laser was set at 391.5 nm to populate N_2^+

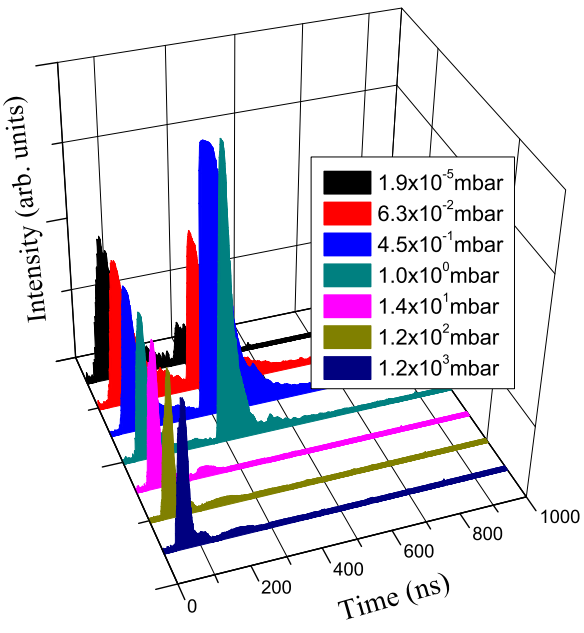

FIG. 4. (Color online) Fluorescence and LIF decay at different gas pressures. The intensities have been normalized with the fluorescence intensity. In the measurement, the nanosecond laser wavelength was set at 391.5 nm, and the collecting fluorescence wavelength was set at 427.8 nm. The time delay between the femtosecond laser and the nanosecond laser was 200 ns. For visual convenience, the decay curves have been shifted backward 30 ns relative to the moment of the femtosecond laser irradiation.

from $X\ ^2\Sigma_g^+(v''=0)$ to $B\ ^2\Sigma_u^+(v'=0)$. The fluorescence wavelength was set at 427.8 nm to collect the fluorescence emission of $N_2^+(B\ ^2\Sigma_u^+, v'=0 \rightarrow X\ ^2\Sigma_g^+, v''=1)$. The time delay between the femtosecond laser and the nanosecond laser was 200 ns. It can be seen that the ratio of the LIF intensity to the fluorescence intensity increased first then decreased with increasing the gas pressure. The observation indicated that the population ratio of $N_2^+(X\ ^2\Sigma_g^+)$ to $N_2^+(B\ ^2\Sigma_u^+)$ increased first then decreased with increasing the gas pressure. It should be emphasized that here the population of $N_2^+(X\ ^2\Sigma_g^+)$ is the population at the moment of 200 ns after the femtosecond laser irradiation.

The population of $N_2^+(X\ ^2\Sigma_g^+)$ was determined by three major reactions under the current experimental condition. First, $N_2^+(X\ ^2\Sigma_g^+)$ was populated through direct ionization of N_2 molecules described by reaction (1). Second, $N_2^+(X\ ^2\Sigma_g^+)$ was populated through collision-induced nonradiative processes of N_2^{+*} described by reaction (3), and N_2^{+*} represents N_2^+ in the excited states. Third, $N_2^+(X\ ^2\Sigma_g^+)$ was depopulated by collision-induced recombination described by reaction (4). These dynamic processes can be expressed as

$$N_2 + \text{laser} \rightarrow N_2^+(X) + e, \quad (1)$$

$$N_2 + \text{laser} \rightarrow N_2^{+*} + e, \quad (2)$$

$$N_2^{+*} + N_2 \rightarrow N_2^+(X) + N_2, \quad (3)$$

$$N_2^+(X) + N_2 \rightarrow N_4^+, \quad (4)$$

$$N_4^+ + e \rightarrow N_2(C\ ^3\Pi_u). \quad (5)$$

When the gas pressure was 1.9×10^{-5} mbar, the mean collision time was very long and up to 8 ms. Thus the collision-induced population and depopulation can be neglected for $N_2^+(X\ ^2\Sigma_g^+)$ at the moment of the nanosecond irradiation. Under this condition, the population of $N_2^+(X\ ^2\Sigma_g^+)$ was mainly determined by the ionization probability of N_2 by intense femtosecond laser fields. State-resolved fluorescence spectra revealed that N_2^+ generated in the laser-induced ionization has a broad vibrational population distribution [41]. However, the nanosecond laser that we applied to populate N_2^+ from $X\ ^2\Sigma_g^+$ to $B\ ^2\Sigma_u^+$ has a narrow bandwidth. The N_2^+ only in $X\ ^2\Sigma_g^+(v''=0)$ can be populated to $B\ ^2\Sigma_u^+(v'=0)$ when the wavelength was set at 391.5 nm for the nanosecond laser. Thus the pumping efficiency was very low. The low population of $N_2^+(B\ ^2\Sigma_u^+, v'=0)$ formed by the nanosecond laser led to the weak LIF, which was consistent with our observation at a very low gas pressure of 1.9×10^{-5} mbar. When the gas pressure was increased to a few millibars, the mean collision time was shortened to tens of nanoseconds. Under this condition, the collision effect on the population of $X\ ^2\Sigma_g^+(v''=0)$ must be taken into account. It is well known that collision is efficient for energy transfer. The vibrational population will relax to $v''=0$ through collision. Thus, the population of $N_2^+(X\ ^2\Sigma_g^+, v''=0)$ will be greatly enhanced at the moment of the nanosecond laser irradiation. Correspondingly, the population of $N_2^+(B\ ^2\Sigma_u^+, v'=0)$ formed by the nanosecond laser will be greatly enhanced. As a result, the LIF intensity will be greatly enhanced. In addition, the N_2^+ in the excited electronic state will relax to the ground electronic state through collisions. For example, the radiative lifetime of $N_2^+(A\ ^2\Pi_u \rightarrow X\ ^2\Sigma_g^+)$ is longer than 10 μs [42]. Collision-induced nonradiative processes will greatly shorten this relax process and will increase the population of $N_2^+(X\ ^2\Sigma_g^+)$ at the moment of the nanosecond laser irradiation. All these collision-induced population redistributions will increase the population of $N_2^+(X\ ^2\Sigma_g^+)$ and thus the LIF intensity. The enhanced LIF intensities at these pressures were consistent with our observations too. When the gas pressure was higher than 1.4×10^1 mbar, the mean collision time became shorter than 10 ns. Thus, there were tens of collisions before the nanosecond laser irradiation. The collision between $N_2^+(X\ ^2\Sigma_g^+)$ and N_2 forms N_4^+. The dissociative recombination of N_4^+ and an electron generates N_2 in the excited electronic state of $C\ ^3\Pi_u$ [39]. The observed emission of $N_2(C\ ^3\Pi_u \rightarrow B\ ^3\Pi_g)$ supports the proposal of the dissociative recombination of N_4^+ and the electron. The dissociative recombination channel greatly depletes the population of $N_2^+(X\ ^2\Sigma_g^+)$ before the nanosecond laser irradiation. As a result, the LIF intensity greatly decreased, which agreed with our experimental observation that the LIF signal dropped fast as the gas pressure was higher than 1.4×10^1 mbar.

The laser-molecule interaction is very complicated, and many reaction channels compete with each other when molecules are subject to intense laser fields. Precise experimental data are essential to reveal the mechanism behind the laser-molecule interaction. The LIF can determine the vibrational population of molecular ions in the ground electronic state. This information can be used to explore the nuclear motion during the process of tunneling ionization of molecules. The combination of fluorescence spectra and LIF spectra can determine the electronic state, whether the molecular ion is in the excited electronic state or the ground electronic state. As a result, the tunneling ionization contributions can be disentangled for different molecular orbitals. The precise experimental data of the ionization probabilities of individual orbitals are very important not only for imaging molecular orbitals, but also for testing the effectiveness of strong-field theoretical models. However, spectroscopic experiments are often carried out at high gas pressures because of the low detection efficiency. Under this condition, the initial population might be changed due to collision at high gas pressures.

IV. CONCLUSIONS

To summarize, we experimentally investigated the tunneling ionization of nitrogen molecules in intense femtosecond laser fields. The N_2^+ ions in the excited electronic states were detected through measuring the fluorescence emission of $N_2^+(B\ ^2\Sigma_u^+ \rightarrow X\ ^2\Sigma_g^+)$. The fluorescence lifetime was observed to decrease with increasing the gas pressure. This observation demonstrated that collision depopulates the excited electronic state and shortens the lifetime of N_2^+ in the excited electronic state. The N_2^+ ions in the ground electronic states were detected through measuring the LIF. The ratio of the LIF intensity to the fluorescence intensity was obtained as a function of gas pressure. The results demonstrated that the ratio increased first then decreased as the gas pressure increased. The gas-pressure dependence of LIF was well

explained by the collision-induced population redistribution in the ground electronic states. The present study demonstrated that the combination of fluorescence spectra and LIF spectra can determine the electronic state of molecular ions. Therefore the spectroscopic method is effective to isolate the contribution of individual molecular orbitals in the tunneling ionization of molecules. In addition, the present study also demonstrated that the collision-induced population redistribution should be taken into account when exploring the population inversion between $N_2^+(B\ ^2\Sigma_u^+)$ and $N_2^+(X\ ^2\Sigma_g^+)$ that has been observed in the interaction of nitrogen molecules and intense laser fields.

ACKNOWLEDGMENTS

This work was supported by the National Basic Research Program of China (Grant No. 2013CB922403), the National Natural Science Foundation of China (Grants No. 61178019, No. 11134001, and No. 11121091), and the program for New Century Excellent Talents in University of China.

[1] K. Yamanouchi, Science **295**, 1659 (2002).
[2] P. B. Corkum, Phys. Rev. Lett. **71**, 1994 (1993).
[3] G. G. Paulus, F. Grasbon, H. Walther, P. Villoresi, M. Nisoli, S. Stagira, E. Priori, and S. De Silvestri, Nature (London) **414**, 182 (2001).
[4] J. Itatani, J. Levesque, D. Zeidler, H. Niikura, H. Pépin, J. C. Kieffer, P. B. Corkum, and D. M. Villeneuve, Nature (London) **432**, 867 (2004).
[5] A. S. Alnaser, S. Voss, X.-M. Tong, C. M. Maharjan, P. Ranitovic, B. Ulrich, T. Osipov, B. Shan, Z. Chang, and C. L. Cocke, Phys. Rev. Lett. **93**, 113003 (2004).
[6] M. Meckel, D. Comtois, D. Zeidler, A. Staudte, D. Pavičić, H. C. Bandulet, H. Pépin, J. C. Kieffer, R. Dörner, D. M. Villeneuve, and P. B. Corkum, Science **320**, 1478 (2008).
[7] H. Niikura, F. Legare, R. Hasbani, A. D. Bandrauk, M. Y. Ivanov, D. M. Villeneuve, and P. B. Corkum, Nature (London) **417**, 917 (2002).
[8] H. Niikura, F. Legare, R. Hasbani, A. D. Bandrauk, M. Y. Ivanov, D. M. Villeneuve, and P. B. Corkum, Nature (London) **421**, 826 (2003).
[9] C. Wu, C. Wu, Y. Yang, Z. Wu, X. Liu, X. Xie, H. Liu, Y. Deng, Y. Liu, H. Jiang, and Q. Gong, J. Mod. Opt. **60**, 1388 (2013).
[10] O. Smirnova, Y. Mairesse, S. Patchkovskii, N. Dudovich, D. Villeneuve, P. Corkum, and M. Y. Ivanov, Nature (London) **460**, 972 (2009).
[11] H. Akagi, T. Otobe, A. Staudte, A. Shiner, F. Turner, R. Dörner, D. M. Villeneuve, and P. B. Corkum, Science **325**, 1364 (2009).
[12] C. Cornaggia, J. Lavancier, D. Normand, J. Morellec, and H. X. Liu, Phys. Rev. A **42**, 5464 (1990).
[13] C. L. Guo, M. Li, and G. N. Gibson, Phys. Rev. Lett. **82**, 2492 (1999).
[14] J. P. Nibarger, S. V. Menon, and G. N. Gibson, Phys. Rev. A **63**, 053406 (2001).
[15] Z. X. Zhao, X. M. Tong, and C. D. Lin, Phys. Rev. A **67**, 043404 (2003).
[16] S. Voss, A. S. Alnaser, X. M. Tong, C. M. Maharjan, P. Ranitovic, B. Ulrich, B. Shan, Z. Chang, and C. L. Cocke, J. Phys. B: At., Mol. Opt. Phys. **37**, 4239 (2004).
[17] E. Baldit, S. Saugout, and C. Cornaggia, Phys. Rev. A **71**, 021403(R) (2005).
[18] R. N. Coffee and G. N. Gibson, Phys. Rev. A **72**, 011401(R) (2005).
[19] J. Huang, C. Wu, N. Xu, Q. Liang, Z. Wu, H. Yang, and Q. Gong, J. Phys. Chem. A **110**, 10179 (2006).
[20] J. McKenna, M. Suresh, B. Srigengan, I. D. Williams, W. A. Bryan, E. M. L. English, S. L. Stebbings, W. R. Newell, I. C. E. Turcu, J. M. Smith, E. J. Divall, C. J. Hooker, A. J. Langley, and J. L. Collier, Phys. Rev. A **73**, 043401 (2006).
[21] D. Pavičić, K. F. Lee, D. M. Rayner, P. B. Corkum, and D. M. Villeneuve, Phys. Rev. Lett. **98**, 243001 (2007).
[22] J. Liu, D. F. Ye, J. Chen, and X. Liu, Phys. Rev. Lett. **99**, 013003 (2007).
[23] W. Guo, J. Y. Zhu, B. X. Wang, Y. Q. Wang, and L. Wang, Phys. Rev. A **77**, 033415 (2008).
[24] Z. Wu, C. Wu, X. Liu, Y. Deng, Q. Gong, D. Song, and H. Su, J. Phys. Chem. A **114**, 6751 (2010).
[25] S. Petretti, Y. V. Vanne, A. Saenz, A. Castro, and P. Decleva, Phys. Rev. Lett. **104**, 223001 (2010).
[26] C. Wu, Y. Yang, Z. Wu, B. Chen, H. Dong, X. Liu, Y. Deng, H. Liu, Y. Liu, and Q. Gong, Phys. Chem. Chem. Phys. **13**, 18398 (2011).
[27] X. M. Tong, Z. X. Zhao, and C. D. Lin, Phys. Rev. A **66**, 033402 (2002).
[28] B. K. McFarland, J. P. Farrell, P. H. Bucksbaum, and M. Gühr, Science **322**, 1232 (2008).
[29] S. Haessler, J. Caillat, W. Boutu, C. Giovanetti-Teixeira, T. Ruchon, T. Auguste, Z. Diveki, P. Breger, A. Maquet, B. Carre, R. Taieb, and P. Salieres, Nat. Phys. **6**, 200 (2010).
[30] Y.-C. Wang, C.-Y. Wu, Y.-X. Liu, S.-H. Xu, and Q.-H. Gong, Front. Phys. **8**, 34 (2013).
[31] J. Yao, B. Zeng, H. Xu, G. Li, W. Chu, J. Ni, H. Zhang, S. L. Chin, Y. Cheng, and Z. Xu, Phys. Rev. A **84**, 051802(R) (2011).
[32] W. Chu, B. Zeng, J. Yao, H. Xu, J. Ni, G. Li, H. Zhang, F. He, C. Jing, Y. Cheng, and Z. Xu, Europhys. Lett. **97**, 64004 (2012).
[33] J. Ni, W. Chu, C. Jing, H. Zhang, B. Zeng, J. Yao, G. Li, H. Xie, C. Zhang, H. Xu, S. L. Chin, Y. Cheng, and Z. Xu, Opt. Express **21**, 8746 (2013).
[34] J. Yao, G. Li, C. Jing, B. Zeng, W. Chu, J. Ni, H. Zhang, H. Xie, C. Zhang, H. Li, H. Xu, S. L. Chin, Y. Cheng, and Z. Xu, New J. Phys. **15**, 023046 (2013).
[35] H. Zhang, C. Jing, J. Yao, G. Li, B. Zeng,W. Chu, J. Ni, H. Xie, H. Xu, S. L. Chin, K. Yamanouchi, Y. Cheng, and Z. Xu, Phys. Rev. X **3**, 041009 (2013).
[36] W. Chu, G. Li, H. Xie, J. Ni, J. Yao, B. Zeng, H. Zhang, C. Jing, H. Xu, Y. Cheng, and Z. Xu, Laser Phys. Lett. **11**, 015301 (2014).
[37] Y. Liu, Y. Brelet, G. Point, A. Houard, and A. Mysyrowicz, Opt. Express **21**, 22791 (2013).
[38] C. Wu, H. Zhang, H. Yang, Q. Gong, D. Song, and H. Su, Phys. Rev. A **83**, 033410 (2011).

[39] H. Xu, A. Azarm, J. Bernhardt, Y. Kamali, and S. L. Chin, Chem. Phys. **360**, 171 (2009).

[40] A. Al-Khalili, H. Ludwigs, and P. Royen, Chem. Phys. Lett. **284**, 191 (1998).

[41] J. Plenge, A. Wirsing, C. Raschpichler, M. Meyer, and E. Rühl, J. Chem. Phys. **130**, 244313 (2009).

[42] B. Yan and W. Feng, Chin. Phys. B **19**, 033303 (2010).